INTERNATIONAL JOURNAL FOR NUMERICAL METHODS IN FLUIDS
Int. J. Numer. Meth. Fluids **31**: 3–15 (1999)

NEW APPROACHES TO ERROR ESTIMATION AND ADAPTIVITY FOR THE STOKES AND OSEEN EQUATIONS

J.T. ODEN* AND S. PRUDHOMME

Texas Institute for Computational and Applied Mathematics, The University of Texas at Austin, Taylor Hall TAY 2.400, Austin, TX 78712, USA

SUMMARY

We present a new approach to deliver reliable approximations of the norm of the residuals resulting from finite element solutions to the Stokes and Oseen equations. The method is based upon a global solve in a bubble space using iterative techniques. This provides an alternative to the classical equilibrated element residual methods for which it is necessary to construct proper boundary conditions for each local problem. The method is first used to develop a global *a posteriori* error estimator. It is then applied in a strategy to control the numerical error in specific outputs or quantities of interest which are functions of the solutions to the Stokes and Oseen equations. Copyright © 1999 John Wiley & Sons, Ltd.

KEY WORDS: error estimation; finite element solutions; Stokes and Oseen equations

1. INTRODUCTION

In recent years, the goal in *a posteriori* error estimation for computational processes has drifted from evaluating the numerical error in the classical energy norm to estimating it in terms of quantities of practical interest. Works in this field have been undertaken in [1–3] with the objective to estimate and/or control the error by adapting the mesh parameters with respect to these quantities. The methodology, developed in [4], is extended here to non-self-adjoint problems, specifically the Oseen equations. It is based on the computation of functions which relate the influence of the residuals, viewed as the sources of error in the finite element approximations, onto the error quantity of interest. However, this technique relies on accurate evaluation of the norm of the residuals and on global error estimators in the 'energy' norm. We then propose a method which belongs to the family of *Implicit Error Residual methods*, for which norms of the residuals $\mathscr{R}_h^m$ in the momentum equation and $\mathscr{R}_h^c$ in the continuity equation are post-processed to provide meaningful error estimates. The computation of the norm of $\mathscr{R}_h^c$ is shown to be exact and cheap. The calculation of the norm of $\mathscr{R}_h^m$ is however more demanding. A new technique is developed which provides accurate approximations of $\mathscr{R}_h^m$ in a space of bubble functions which is gradually enriched through a global but inexpensive iterative process.

* Correspondence to: Texas Institute for Computational and Applied Mathematics, The University of Texas at Austin, Taylor Hall TAY 2.400, Austin, TX 78712, USA.

CCC 0271–2091/99/170003–13$17.50

2. PRELIMINARIES AND NOTATION

Let Ω denote an open bounded Lipschitz domain in $\mathbb{R}^d$, $d=2$ or 3, with boundary $\partial\Omega$. We consider the Oseen equations with homogeneous boundary conditions:

$$\begin{aligned} &-\Delta \boldsymbol{u} + (\boldsymbol{\alpha}\cdot\nabla)\boldsymbol{u} + \nabla p = \boldsymbol{f} \quad \text{in } \Omega \\ &\nabla\cdot\boldsymbol{u} = 0 \quad \text{in } \Omega \\ &\boldsymbol{u} = \boldsymbol{0} \quad \text{on } \partial\Omega, \end{aligned} \tag{2.1}$$

where $\boldsymbol{u}=\boldsymbol{u}(\boldsymbol{x})$ and $p=p(\boldsymbol{x})$ are the velocity and pressure defined at point $\boldsymbol{x}=(x_1, x_2, \ldots, x_n)$ in Ω and $\boldsymbol{\alpha}$ is a smooth divergence-free vector field on Ω (i.e. $\nabla\cdot\boldsymbol{\alpha}=0$). The source term $\boldsymbol{f}=\boldsymbol{f}(\boldsymbol{x})$ is a prescribed body force. The Stokes equations are recovered from the Oseen equations by setting $\boldsymbol{\alpha}=\boldsymbol{0}$.

We begin by introducing the trial spaces of velocities $\boldsymbol{V}$ and pressures Q defined by:

$$\boldsymbol{V} = \boldsymbol{H}_0^1(\Omega) = (H_0^1(\Omega))^d, \qquad Q = \left\{ q\in L^2(\Omega): \int_\Omega q \, \mathrm{d}x = 0 \right\},$$

with corresponding norms:

$$|\boldsymbol{v}|_1^2 = \int_\Omega \nabla\boldsymbol{v}:\nabla\boldsymbol{v} \, \mathrm{d}x, \qquad \|q\|_0^2 = \int_\Omega q^2 \, \mathrm{d}x.$$

We also introduce the bilinear forms a, b and c:

$$\begin{aligned} &a:\ \boldsymbol{H}^1(\Omega)\times\boldsymbol{H}^1(\Omega)\to\mathbb{R}; \quad a(\boldsymbol{u},\boldsymbol{v}) = \int_\Omega \nabla\boldsymbol{u}:\nabla\boldsymbol{v} \, \mathrm{d}x, \\ &b:\ \boldsymbol{H}^1(\Omega)\times L^2(\Omega)\to\mathbb{R}; \quad b(\boldsymbol{v},q) = -\int_\Omega q\nabla\cdot\boldsymbol{v} \, \mathrm{d}x, \\ &c:\ \boldsymbol{H}^1(\Omega)\times\boldsymbol{H}^1(\Omega)\to\mathbb{R}; \quad c(\boldsymbol{\alpha};\boldsymbol{u},\boldsymbol{v}) = \int_\Omega (\boldsymbol{\alpha}\cdot\nabla)\boldsymbol{u}\cdot\boldsymbol{v} \, \mathrm{d}x \end{aligned}$$

and consider the bilinear form $\tilde{a}$

$$\tilde{a}(\boldsymbol{u},\boldsymbol{v}) = a(\boldsymbol{u},\boldsymbol{v}) + c(\boldsymbol{\alpha};\boldsymbol{u},\boldsymbol{v}). \tag{2.2}$$

Then, denoting $\boldsymbol{V}'$ the dual space of $\boldsymbol{V}$, the variational formulation of the Oseen and Stokes problems reads:

$$\boxed{\begin{aligned} &\text{For } \boldsymbol{f}\in\boldsymbol{V}' \text{ given, find } (\boldsymbol{u},p)\in\boldsymbol{V}\times Q, \text{ s.t.} \\ &\tilde{a}(\boldsymbol{u},\boldsymbol{v}) + b(\boldsymbol{v},p) = \langle \boldsymbol{f},\boldsymbol{v}\rangle, \quad \forall\boldsymbol{v}\in\boldsymbol{V} \\ &b(\boldsymbol{u},q) = 0, \quad \forall q\in Q \end{aligned}} \tag{2.3}$$

The bilinear forms $\tilde{a}$ and b are continuous with constants $M_{\tilde{a}}$ and M_b respectively. The constant $M_{\tilde{a}}$ depends on the vector $\boldsymbol{\alpha}$, and in particular, is equal to 1 when $\boldsymbol{\alpha}=\boldsymbol{0}$. The constant M_b is equal to $\sqrt{d}$ when $\boldsymbol{v}\in\boldsymbol{H}^1(\Omega)$ [4] and to 1 when $\boldsymbol{v}\in\boldsymbol{H}_0^1(\Omega)$. Moreover, the form $\tilde{a}$ is coercive, as for every $\boldsymbol{v}\in\boldsymbol{H}_0^1(\Omega)$,

$$\tilde{a}(\boldsymbol{v},\boldsymbol{v}) = a(\boldsymbol{v},\boldsymbol{v}) + c(\boldsymbol{\alpha};\boldsymbol{v},\boldsymbol{v}) = a(\boldsymbol{v},\boldsymbol{v}) = |\boldsymbol{v}|_1^2.$$

Moreover, it can be shown that b satisfies the standard LBB condition [5], in the sense that there exists a constant $\beta>0$ such that:

$$\sup_{\boldsymbol{v}\in\boldsymbol{V}\setminus\{0\}} \frac{|b(\boldsymbol{v}, q)|}{|\boldsymbol{v}|_1} \geq \beta \|q\|_0, \quad \forall q\in Q. \tag{2.4}$$

Then, it is well-known that problem (2.3) admits a unique solution $(\boldsymbol{u}, p)$ in $\boldsymbol{V}\times Q$ (see for example [5]).

Let $\boldsymbol{V}^h$ and Q^h denote two conforming finite element subspaces, possibly h–p finite element spaces [6], of $\boldsymbol{V}$ and Q in the sense that $\boldsymbol{V}^h\subset\boldsymbol{V}$ and $Q^h\subset Q$. Then, the finite element problem provides approximate solutions $(\boldsymbol{u}_h, p_h)\in\boldsymbol{V}^h\times Q^h$ of $(\boldsymbol{u}, p)$:

$$\boxed{\begin{array}{l}\text{For } \boldsymbol{f}\in\boldsymbol{V}' \text{ given, find } (\boldsymbol{u}_h, p_h)\in\boldsymbol{V}^h\times Q^h, \text{ s.t.}\\ \tilde{a}(\boldsymbol{u}_h, \boldsymbol{v}) + b(\boldsymbol{v}, p_h) = \langle \boldsymbol{f}, \boldsymbol{v}\rangle, \quad \forall \boldsymbol{v}\in\boldsymbol{V}^h\\ b(\boldsymbol{u}_h, q) = 0, \quad \forall q\in Q^h\end{array}} \tag{2.5}$$

3. GLOBAL ERROR ESTIMATION

We recall that the goal in global error estimation is to obtain a global measure of the numerical error over the whole domain Ω. Since a direct computation of the error is to be avoided, due to the prohibitive cost, the choice of an appropriate measure is generally suggested by the problem itself. Following is a brief review of the methodology for the Oseen equations presented by Oden and Prudhomme [4] for the Stokes problem.

Let $(\boldsymbol{e}, E) = (\boldsymbol{u}-\boldsymbol{u}_h, p-p_h)\in\boldsymbol{V}\times Q$ define the numerical error in the finite element solution $(\boldsymbol{u}_h, p_h)$. Replacing $\boldsymbol{u}$ and p in (2.3) by $(\boldsymbol{u}_h+\boldsymbol{e})$ and (p_h+E), the error $(\boldsymbol{e}, E)$, due to the finite element discretization, satisfies the system of equations:

$$\boxed{\begin{array}{l}\tilde{a}(\boldsymbol{e}, \boldsymbol{v}) + b(\boldsymbol{v}, E) = \mathscr{R}_h^m(\boldsymbol{v}), \quad \forall \boldsymbol{v}\in\boldsymbol{V}\\ b(\boldsymbol{e}, q) = \mathscr{R}_h^c(q), \quad \forall q\in Q\end{array}} \tag{3.6}$$

where the linear functionals $\mathscr{R}_h^m\colon \boldsymbol{V}\to\mathbb{R}$ and $\mathscr{R}_h^c\colon Q\to\mathbb{R}$,

$$\mathscr{R}_h^m(\boldsymbol{v}) = \langle \mathscr{R}_h^m, \boldsymbol{v}\rangle \equiv \langle \boldsymbol{f}, \boldsymbol{v}\rangle - \tilde{a}(\boldsymbol{u}_h, \boldsymbol{v}) - b(\boldsymbol{v}, p_h)$$
$$\mathscr{R}_h^c(q) = \langle \mathscr{R}_h^c, q\rangle \equiv -b(\boldsymbol{u}_h, q)$$

are the residuals in the *momentum equation* and *continuity equation*, respectively. The residuals $\mathscr{R}_h^m$ and $\mathscr{R}_h^c$ represent the *source terms of the error*. As such, we shall show that they deliver equivalent measures of the error for appropriate choices of norms.

The norms of the residuals are defined as:

$$\|\mathscr{R}_h^m\|_* = \sup_{\boldsymbol{v}\in\boldsymbol{V}\setminus\{\boldsymbol{0}\}} \frac{\mathscr{R}_h^m(\boldsymbol{v})}{|\boldsymbol{v}|_1}, \qquad \|\mathscr{R}_h^c\|_* = \sup_{q\in Q\setminus\{0\}} \frac{\mathscr{R}_h^c(q)}{\|q\|_0}. \tag{3.7}$$

We can then prove the following theorem (see [4]):

Theorem 3.1
With above definitions

$$C_1(|\boldsymbol{e}|_1^2 + \|E\|_0^2) \leq \|\mathscr{R}_h^c\|_*^2 + \|\mathscr{R}_h^m\|_*^2 \leq C_2(|\boldsymbol{e}|_1^2 + \|E\|_0^2), \tag{3.8}$$

where C_1 and C_2 are two positive constants depending, respectively, on $M_{\tilde{a}}$ and β, and, on $M_{\tilde{a}}$ and M_b.

The global quantity $\|\mathscr{R}_h^m\|_*^2 + \|\mathscr{R}_h^c\|_*^2$ gives a meaningful global estimate of the error as long as the constants C_1 and C_2 remain close to one. For instance, in the case of the Stokes problem, it can be shown that $C_1 = \min(1, \beta^4)$ and $C_2 = \max(2 + M_b^2, 2M_b^2)$. However, we emphasize that such a result does not provide any reliable information about the local error in general, as it is clear that the error may propagate far away from the sources $\mathscr{R}_h^m$ and $\mathscr{R}_h^c$. Nevertheless, elementwise contributions of $\|\mathscr{R}_h^m\|_*$ and $\|\mathscr{R}_h^c\|_*$ can be utilized to derive local refinement indicators in order to reduce the global error in the numerical solution.

The evaluation of $\|\mathscr{R}_h^c\|_*$ is straightforward and exact.

Lemma 3.1
Let $\boldsymbol{u}_h \in \boldsymbol{V}^h$ be the discrete velocity of the Stokes or Oseen equations. Then:

$$\|\mathscr{R}_h^c\|_* = \|\nabla \cdot \boldsymbol{u}_h\|_0. \tag{3.9}$$

On the other hand, only approximations of $\|\mathscr{R}_h^m\|_*$ can be sought:

Theorem 3.2
Let $\tilde{\boldsymbol{V}}^h$, $\boldsymbol{V}^h \subset \tilde{\boldsymbol{V}}^h \subset \boldsymbol{V}$ be a finite element space for which there exists σ, $0 \le \sigma < 1$ such that $|\boldsymbol{\varphi} - \boldsymbol{\varphi}_h|_1 \le \sigma |\boldsymbol{\varphi}|_1$, where $\boldsymbol{\varphi}$ and $\boldsymbol{\varphi}_h$ satisfy:

$$a(\boldsymbol{\varphi}, \boldsymbol{v}) = \mathscr{R}_h^m(\boldsymbol{v}), \quad \forall \boldsymbol{v} \in \boldsymbol{V}, \tag{3.10}$$

$$a(\boldsymbol{\varphi}_h, \boldsymbol{v}) = \mathscr{R}_h^m(\boldsymbol{v}), \quad \forall \boldsymbol{v} \in \tilde{\boldsymbol{V}}^h. \tag{3.11}$$

Let $\tilde{\boldsymbol{V}}^h$ be decomposed as $\tilde{\boldsymbol{V}}^h = \boldsymbol{V}^h + \boldsymbol{W}^h$ such that a strengthened Cauchy–Schwartz inequality holds [7], i.e. there exists γ, $0 \le \gamma < 1$, such that $a(\boldsymbol{v}_h, \boldsymbol{w}_h) \le \gamma |\boldsymbol{v}_h|_1 |\boldsymbol{w}_h|_1$, for all $\boldsymbol{v}_h \in \boldsymbol{V}^h$ and $\boldsymbol{w}_h \in \boldsymbol{W}^h$. Then

$$\sqrt{(1-\sigma^2)(1-\gamma^2)}\,\|\mathscr{R}_h^m\|_* \le |\boldsymbol{\psi}_h|_1 \le \|\mathscr{R}_h^m\|_*, \tag{3.12}$$

where $\boldsymbol{\psi}_h \in \boldsymbol{W}^h$ is the solution of the finite system

$$a(\boldsymbol{\psi}_h, \boldsymbol{v}) = \mathscr{R}_h^m(\boldsymbol{v}), \quad \forall \boldsymbol{v} \in \boldsymbol{W}^h. \tag{3.13}$$

For the proofs of this lemma and theorem, we refer to Oden and Prudhomme [4]. The accuracy in $|\boldsymbol{\psi}_h|_1$ of $\|\mathscr{R}_h^m\|_*$ depends on σ and γ. In our h–p code used in the numerical experiment to be discussed later, the basis functions are constructed via a family of hierarchic shape functions based on the integrated Legendre polynomials (see [8]). Most of these shape functions are orthogonal to each other with respect to the inner product $a(\cdot, \cdot)$ (see [9]), which allows us to stipulate that the constant γ should be close to 0.

On the other hand, the constant σ depends on the richness of $\boldsymbol{W}^h$. The space of perturbations $\boldsymbol{W}^h$ is constructed from layers of basis functions of degree between $p+1$ and $p+q$, $q \ge 1$, where p is the maximal degree of the shape functions in $\boldsymbol{V}^h$ for each element. In h–p finite element methods, these perturbations are viewed as bubble functions. In two-dimensional problems, the functions are either *interior bubbles* whose support reduces to only one element or *edge bubbles* whose support is shared by two contiguous elements. One expects the value of σ to tend to 0 as q increases.

Combining the result of Lemma 3.1 and of Theorems 3.1 and 3.2, one obtains the following estimator η_u:

$$\eta_u^2 = |\boldsymbol{\psi}_h|_1^2 + \|\nabla \cdot \boldsymbol{u}_h\|_0^2. \tag{3.14}$$

Then, from (3.8), (3.9) and (3.12),

$$C_1(1-\sigma^2)(1-\gamma^2)(|e|_1^2+\|E\|_0^2)\le\eta_u^2\le C_2(|e|_1^2+\|E\|_0^2). \tag{3.15}$$

The overall cost of this estimator scales down to the cost in solving the global problem (3.13). We have proposed a coupled iterative procedure, in which the distribution of q is adapted by enriching the space $\boldsymbol{W}^h$ with new bubble functions in those elements where the elementwise contributions to $|\boldsymbol{\psi}_h|_1$ are large, while solving (3.13) by an iterative Conjugate Gradient method (CG) performing only a few iterations. Our approach is therefore different from the *equilibrated residual* method of Ainsworth and Oden [10,11], for which the global problem is decoupled into a collection of elementwise problems, and avoids the major difficulty of prescribing proper (equilibrated) boundary conditions for each subproblem [11,12], at comparable cost. See [4] for a study of the performance of this global error estimator for the Stokes problem.

4. GOAL-ORIENTED ERROR ESTIMATION

A general objective in engineering applications and numerical simulations is to predict specific quantities of interest in terms of the solution $(\boldsymbol{u}, p)$, such as pointwise quantities, drag and lift coefficients, flow rates, etc. For instance, let us suppose we want to predict a quantity $L(\boldsymbol{u}, p)$, where L represents a linear functional of $(\boldsymbol{u}, p)$. Then the computational process should be designed in such a way that it controls the error quantity $L(\boldsymbol{e}, E)=L(\boldsymbol{u}-\boldsymbol{u}_h, p-p_h)$, rather than the global error measure $|\boldsymbol{e}|_1^2+\|E\|_0^2$.

The starting point of goal-oriented error estimation is as follows: since the residuals $\mathscr{R}_h^m$ and $\mathscr{R}_h^c$ represent the sources of errors, we would like to find linear functionals $\boldsymbol{\omega}^m$ and ω^c, if they exist, such that:

$$L(\boldsymbol{e}, E)=\boldsymbol{\omega}^m(\mathscr{R}_h^m)+\omega^c(\mathscr{R}_h^c). \tag{4.16}$$

These functions are named *influence functions* as they indicate the influence of the residuals on the quantity $L(e, E)$. They are defined on the bidual of $\boldsymbol{V}$ and Q, and since these spaces are reflexive, the relation (4.16) becomes:

$$L(\boldsymbol{e}, E)=\mathscr{R}_h^m(\boldsymbol{\omega}^m)+\mathscr{R}_h^c(\omega^c). \tag{4.17}$$

Substituting for the terms $\mathscr{R}_h^m(\boldsymbol{\omega}^m)$ and $\mathscr{R}_h^c(\omega^c)$ in (4.17) using (3.6), one gets:

$$L(\boldsymbol{e}, E)=\tilde{a}(\boldsymbol{e}, \boldsymbol{\omega}^m)+b(\boldsymbol{\omega}^m, E)+b(\boldsymbol{e}, \omega^c). \tag{4.18}$$

It follows that the influence functions can be obtained as solutions of the global *dual problem*:

$$\begin{aligned}&\text{Find } (\boldsymbol{\omega}^m, \omega^c)\in\boldsymbol{V}\times Q, \text{ such that}\\ &\tilde{a}(\boldsymbol{v}, \boldsymbol{\omega}^m)+b(\boldsymbol{v}, \omega^c)+b(\boldsymbol{\omega}^m, q)=L(\boldsymbol{v}, q), \quad \forall(\boldsymbol{v}, q)\in\boldsymbol{V}\times Q\end{aligned} \tag{4.19}$$

which may be rewritten:

$$\begin{aligned}&\text{Find } (\boldsymbol{\omega}^m, \omega^c)\in\boldsymbol{V}\times Q, \text{ such that}\\ &\tilde{a}(\boldsymbol{v}, \boldsymbol{\omega}^m)+b(\boldsymbol{v}, \omega^c)=L(\boldsymbol{v}, 0), \quad \forall\boldsymbol{v}\in\boldsymbol{V}\\ &\boldsymbol{b}(\boldsymbol{\omega}^m, q)=L(\boldsymbol{0}, q), \quad \forall q\in Q\end{aligned} \tag{4.20}$$

It readily follows that the functions $\boldsymbol{\omega}^m$ and ω^c do exist and are unique as $L(\boldsymbol{v}, 0) \in \boldsymbol{V}'$ and $L(\boldsymbol{0}, q) \in Q'$ (see [5]).

Obviously, problem (4.20) cannot be solved exactly for the functions $\boldsymbol{\omega}^m$ and ω^c in the general case. Instead, one computes finite element approximations $\boldsymbol{\omega}_h^m$ and ω_h^c of $\boldsymbol{\omega}^m$ and ω^c, respectively, in the solution space $\boldsymbol{V}^h \times Q^h$ by the Galerkin method, that is:

$$\boxed{\begin{aligned} &\text{Find } (\boldsymbol{\omega}_m^h, \omega_h^c) \in \boldsymbol{V}^h \times Q^h, \text{ such that} \\ &\tilde{a}(\boldsymbol{v}, \boldsymbol{\omega}_h^m) + b(\boldsymbol{v}, \omega_h^c) = L(\boldsymbol{v}, 0), \quad \forall \boldsymbol{v} \in \boldsymbol{V}^h \\ &b(\boldsymbol{\omega}_h^m, q) = L(\boldsymbol{0}, q), \quad \forall q \in Q^h \end{aligned}} \tag{4.21}$$

Observing from the definition of the residuals that

$$\mathscr{R}_h^m(\boldsymbol{\omega}_h^m) = 0, \qquad \mathscr{R}_h^c(\omega_h^c) = 0, \tag{4.22}$$

one gets from (4.17),

$$L(\boldsymbol{e}, E) = \mathscr{R}_h^m(\boldsymbol{\omega}^m) + \mathscr{R}_h^c(\omega^c) = \mathscr{R}_h^m(\boldsymbol{\omega}^m - \boldsymbol{\omega}_h^m) + \mathscr{R}_h^c(\omega^c - \omega_h^c). \tag{4.23}$$

Denoting the numerical error $(\boldsymbol{\varepsilon}, \xi) = (\boldsymbol{\omega}^m - \boldsymbol{\omega}_h^m, \omega^c - \omega_h^c)$ in the influence functions, which naturally satisfies the system of equations:

$$\boxed{\begin{aligned} &\tilde{a}(\boldsymbol{v}, \boldsymbol{\varepsilon}) + b(\boldsymbol{v}, \xi) = \bar{\mathscr{R}}_h^m(\boldsymbol{v}), \quad \forall \boldsymbol{v} \in \boldsymbol{V} \\ &b(\boldsymbol{\varepsilon}, q) = \bar{\mathscr{R}}_h^c(q), \quad \forall q \in Q \end{aligned}} \tag{4.24}$$

where $\bar{\mathscr{R}}_h^m(\boldsymbol{v}) = L(\boldsymbol{v}, 0) - \tilde{a}(\boldsymbol{v}, \boldsymbol{\omega}_h^m) - b(\boldsymbol{v}, \omega_h^c)$ and $\bar{\mathscr{R}}_h^c(q) = L(\boldsymbol{0}, q) - b(\boldsymbol{\omega}_h^m, q)$ are the residuals associated with the influence functions, we then have after simplifications

$$\begin{aligned} |L(\boldsymbol{e}, E)| = |\mathscr{R}_h^m(\boldsymbol{\varepsilon}) + \mathscr{R}_h^c(\xi)| &= |a(\boldsymbol{\varphi}, \boldsymbol{\varepsilon}) - b(\boldsymbol{u}_h, \xi)| \le \sum_K |a_K(\boldsymbol{\varphi}, \boldsymbol{\varepsilon})| + |b_K(\boldsymbol{u}_h, \xi)| \\ &\le \sum_K |\varphi|_{1,K} |\boldsymbol{\varepsilon}|_{1,K} + \|\nabla \cdot \boldsymbol{u}_h\|_{0,K} \|\xi\|_{0,K} \qquad (4.25) \\ &\le \sum_K \sqrt{|\boldsymbol{\varphi}|_{1,K}^2 + \|\nabla \cdot \boldsymbol{u}_h\|_{0,K}^2} \sqrt{|\boldsymbol{\varepsilon}|_{1,K}^2 + \|\xi\|_{0,K}^2}. \qquad (4.26) \end{aligned}$$

We recall that $\boldsymbol{\varphi}$ is the function in $\boldsymbol{V}$ satisfying (3.10). The symbol Σ_K refers to the summation over all elements $K = 1, \ldots, N_e$ in the mesh, and the subscript K attached to the norms or the bilinear forms a and b denote restrictions of the associated global quantity to an element K in the mesh.

Again, the quantities on the right-hand side of inequality (4.26) cannot be determined exactly. Therefore we resort to the techniques developed in the previous section to find reliable approximations. For example, the function $\boldsymbol{\varphi} \in \boldsymbol{V}$ is approximated by $\boldsymbol{\psi}_h \in \boldsymbol{W}^h$, as shown in Theorem 3.2. The quantity $|\boldsymbol{\varepsilon}|_{1,K}^2 + \|\xi\|_{0,K}^2$ is estimated using the global error estimator since the error $(\boldsymbol{\varepsilon}, \xi)$ in the influence functions satisfies a system of equations similar to the one for the error $(\boldsymbol{e}, E)$ in the numerical solution $(\boldsymbol{u}_h, p_h)$. However, this estimator is in essence global and not local, meaning that it provides a good estimate of the global error $|\boldsymbol{\varepsilon}|_1^2 + \|\xi\|_0^2$, but not necessarily a good estimate of the local quantity $|\boldsymbol{\varepsilon}|_{1,K}^2 + \|\xi\|_{0,K}^2$, due to pollution or propagation errors. Nevertheless, the local estimates improve as the mesh is refined since the pollution effects diminish accordingly.

Therefore, denoting $\eta_{u,K}^2 = |\psi_h|_{0,K}^2 + \|\nabla\cdot\boldsymbol{u}_h\|_{0,K}^2$, and $\eta_{\omega,K}^2$ the estimate for $|\varepsilon|_{1,K}^2 + \|\xi\|_{0,K}^2$, we define the new estimate for $L(e, E)$ as:

$$\eta_L = \sum_K \eta_{u,K}\,\eta_{\omega,K}. \tag{4.27}$$

Rigorously, it cannot be shown that η_L is greater than $|L(e, E)|$. However, in practice, and due to the several inequalities introduced to obtain (4.26), it has been observed that:

$$|L(e, E)| \ll \eta_L. \tag{4.28}$$

Therefore, the quantity η_L does not necessarily deliver an accurate estimate of $|L(e, E)|$ and for this reason is called an error indicator with respect to the quantity of interest L. This indicator still provides valuable information about the elementwise contributions to $|L(e, E)|$ and as such is used in a goal-oriented refinement strategy as described in the next section.

Becker and Rannacher in [2] developed a similar technique for the steady state Navier–Stokes equations. However, in their approach, they use inequality (4.25) to provide elementwise refinement indicators. Moreover, they estimate the residuals by local techniques and resort to local interpolation properties to evaluate the error in the influence functions $|\varepsilon|_{1,K}$ and $\|\xi\|_{0,K}$, introducing an interpolation constant they arbitrarily choose as 1. Another approach has been proposed by Parashivoiu and Patera [13] in order to derive a lower and upper bound to the error quantity $L(e, E)$.

5. ADAPTATIVE STRATEGY TOWARDS ERROR CONTROL

In the previous sections, we presented two techniques to assess the accuracy of finite element solutions of the Stokes and Oseen equations. The first estimates the error in the global norm $(|e|_1^2 + \|E\|_0^2)^{1/2}$, which, from a physical point of view, indicates how the 'energetic sources' of the error are distributed over the whole computational domain. The second technique is more involved than the first, but provides an estimate of the error $L(e, E)$ with respect to a specific goal, expressed in terms of the linear functional L prescribed by the user.

In both cases, the strategy to control the error quantities $(|e|_1^2 + \|E\|_0^2)^{1/2}$ or $L(e, E)$ consists in two steps: (1) check that the relative error is smaller than a preset tolerance C^{tol}; (2) if the tolerance is not satisfied, adapt the finite element mesh in order to reduce the effects of the sources of errors. Then, a new finite element solution is recomputed on the adapted mesh and the new error estimated and controlled. This induces an iterative procedure which terminates once the tolerance is reached.

In the case of the error quantity $(|e|_1^2 + \|E\|_0^2)^{1/2}$, one defines the relative error as:

$$e_{\text{rel}} = \frac{\sqrt{|e|_1^2 + \|E\|_0^2}}{\sqrt{|u|_1^2 + \|p\|_0^2}}. \tag{5.29}$$

Clearly, neither the exact solution (u, p) nor the exact error (e, E) are known. Therefore one checks instead that:

$$\frac{\eta_u}{\sqrt{|u_h|_1^2 + \|p_h\|_0^2}} \leq C^{\text{tol}}, \tag{5.30}$$

where η_u is the error estimator defined in (3.14). Adaptation is performed by refining the elements for which the contributions to η_u are the largest. Decomposing the global quantity η_u into elementwise contributions $\eta_{u,K}$ as:

$$\eta_{u,K}^2 = |\psi_h|_{1,K}^2 + \|\nabla \cdot \boldsymbol{u}_h\|_{0,K}^2, \tag{5.31}$$

so that $\eta_u^2 = \Sigma_K \eta_{u,K}^2$, the indicator for element refinement is given by:

$$\frac{\eta_{u,K}^2}{\max_K (\eta_{u,K}^2)} \geq C^{\text{adp}}, \tag{5.32}$$

where C^{adp} is a number chosen between 0 and 1 depending on the problem (and also on the user's experience). In the numerical experiments presented in the next section, meshes are made up of quadrilateral elements. The refinement procedure consists here in dividing an element into four subquadrilaterals, allowing for 'hanging nodes', as shown in [6]. Alternatively, in the p-version of the finite element method, meshes can be adapted by adding new shape functions of higher degrees in elements verifying the criterion (5.32).

We follow the same strategy to perform the adaptative control of the error quantity $L(\boldsymbol{e}, E)$. In particular we check that

$$\frac{\eta_L}{|L(\boldsymbol{u}_h, p_h)|} \leq C^{\text{tol}} \tag{5.33}$$

in order to decide if refinement is necessary. Here η_L denotes the error indicator as in (4.27). Then, the error $L(\boldsymbol{e}, E)$ can be controlled by refining all the elements for which

$$\frac{\eta_{u,K} \cdot \eta_{\omega,K}}{\max_K (\eta_{u,K} \cdot \eta_{\omega,K})} \geq C^{\text{adp}}, \tag{5.34}$$

where $\eta_{u,K}$ and $\eta_{\omega,K}$ referred to as the elementwise contributions to the estimates of the global quantities $(|\boldsymbol{\varphi}|_1^2 + \|\nabla \cdot \boldsymbol{u}_h\|_0^2)^{1/2}$ and $(|\boldsymbol{\varepsilon}|_1^2 + \|\xi\|_0^2)^{1/2}$, respectively. By doing so, we refine all the elements which contribute the most to the quantity $L(\boldsymbol{e}, E)$.

We conclude this section by a comment on the tolerance C^{tol}, for which the choice (and meaning) of a particular value is somehow ambiguous. On one hand, the relative error based on the global norm $(|\cdot|_1^2 + \|\cdot\|_0^2)^{1/2}$ makes little sense, especially in fluid mechanics. Indeed, for open flow problems, the size of the computational domain Ω is frequently chosen in an arbitrary manner. Meanwhile, the errors may be very large in local regions of the flow, such as corners. It results that the relative error, *a fortiori* the choice of the tolerance, is closely correlated to the size of the domain. In problems of flow over an obstacle, for instance, the relative error can be reduced simply by extending the domain at the inflow (or outflow), though not improving the accuracy of the solution around the obstacle. On the other hand, the relative error based on L has a straightforward meaning for the user as it is related to a specific physical quantity of the solution. Nevertheless, we have pointed out that η_L may overestimate the error $L(\boldsymbol{e}, E)$ by a few orders of magnitude, which implies that the tolerance C^{tol} in (5.33) can not serve as an accurate upper bound of the associated relative error. In conclusion, the adaptative control of the error is fully automatized by just specifying the two parameters C^{tol} and C^{adp}, but the choice of their values still requires proper judgement from the user.

6. NUMERICAL EXAMPLE

The objective of the following numerical experiment is to highlight the advantages of the adaptative process based on quantities of interest L. This is demonstrated on the problem of the channel flow over a surface-mounted obstacle. The computational domain, as well as the initial mesh of 115 elements, are shown in Figure 1, where the obstacle is represented by the unit square $[5, 6] \times [0, 1]$. Along the lateral walls and obstacle, the velocity vector is set to zero.

A Poiseuille-type velocity profile is prescribed at the inflow located on the left side of the domain. At the outflow, we use the artificial boundary condition $-p\boldsymbol{n}+\partial\boldsymbol{u}/\partial n=\boldsymbol{0}$ as in [14] where $\boldsymbol{n}$ denotes the outward normal to the boundary. The velocity and pressure fields are approximated by a piecewise biquadratic and bilinear polynomials respectively. Finally we set $\boldsymbol{\alpha}=\boldsymbol{0}$.

We suppose that the goal of the computations is directed towards the study of the recirculation region upstream of the step. Visualization of the recirculation is generally achieved by plotting the streamlines, which, in two-dimensional flows are the isolines of the streamfunction Ψ, satisfying $u=-\partial\Psi/\partial y$, $v=\partial\Psi/\partial x$. The streamfunction is known to be related to the vorticity $\zeta=\zeta(\boldsymbol{u})$ by the relation

$$\Delta\Psi=\zeta \tag{6.35}$$

so that we choose the quantity of interest to be the *circulation* $\mathscr{C}$ that is, the line integral of the velocity around the closed curve $\partial\Omega_K$ which delimits the fixed subdomain Ω_K as shown in Figure 2. It follows that:

$$L(\boldsymbol{u},p)=\mathscr{C}=\oint_{\partial\Omega_K}\boldsymbol{u}\cdot\mathrm{d}\boldsymbol{s}=\int_{\Omega_K}\zeta(\boldsymbol{u})\,\mathrm{d}x \tag{6.36}$$

where $\mathrm{d}\boldsymbol{s}$ refers to the differential vector along the path of integration $\partial\Omega_K$. For simplicity, the subdomain Ω_K is chosen to coincide with one element of the initial mesh (hence the subscript K). When the mesh is refined, it may then be formed of several subelements. Finally, one remarks that L is a linear functional of the velocity only.

We set up two series of experiments to compare the performance of the adaptation strategy using one or the other error estimators. For the error estimator based on the global 'energy' norm, we set $C^{\mathrm{tol}}=0.00025$ and $C^{\mathrm{adp}}=0.5$. We show in Figures 3 and 5 the adapted meshes after 8 and 14 adaptation cycles. As expected, they exhibit highly refined regions around the top corners of the obstacle due to the large errors produced by the singularity in the pressure. We observe that few elements are refined during the first cycles so that the computations are very cheap in comparison to those performed on the latest meshes. In Figures 4 and 6 we

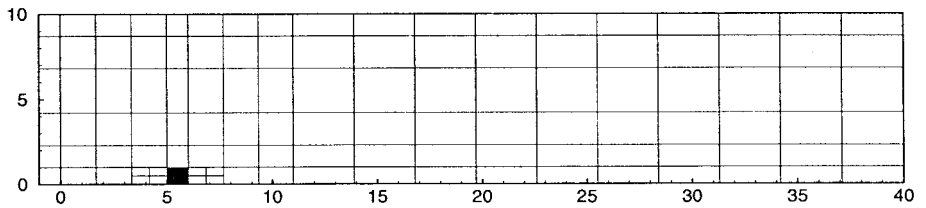

Figure 1. Computational domain and initial mesh for the obstacle problem.

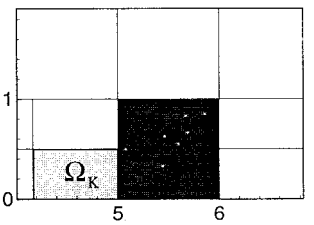

Figure 2. Close-up view of the obstacle and subdomain Ω_K.

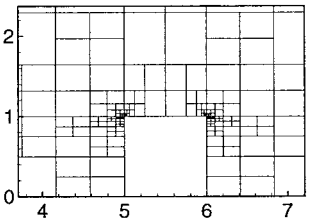

Figure 3. Adapted mesh with 317 elements.

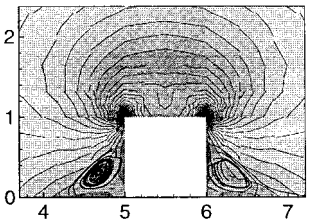

Figure 4. Vorticity contours and streamlines associated with the mesh of Figure 3.

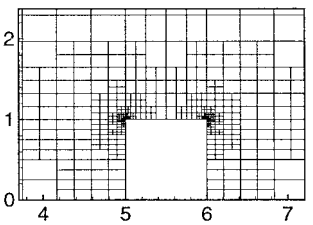

Figure 5. Adapted mesh with 968 elements.

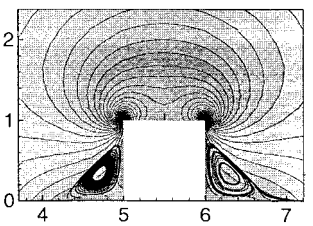

Figure 6. Vorticity contours and streamlines associated with the mesh of Figure 5.

display the vorticity contours and plot the streamlines (actually the pathlines since they are identical for a steady flow), using a visualization package. One observes that these are poorly resolved, even on the finest mesh formed of 968 elements.

In the second series, we adapt the mesh using the estimate based on the error quantity $L(\boldsymbol{e}, E)$ and set $C^{\text{tol}} = 0.1$ and $C^{\text{adp}} = 0.5$. We show in Figure 7 the final mesh obtained after 14 adaptation cycles. It is essentially refined in the subdomain Ω_K, as expected, but also around the upper corners of the obstacle. This shows how much remote sources of errors do influence the recirculation upstream of the obstacle. Such phenomena are regarded as 'pollution effects' by Babuška and coworkers in [1]. We interpret those as the propagation of the error away from the sources of errors $\mathscr{R}_h^m$ and $\mathscr{R}_h^c$. In Figure 8, contour lines of the vorticity and

streamlines are displayed. They compare well qualitatively to the results obtained by Fragos *et al.* [15] as far as the recirculation region upstream of the obstacle is concerned.

Figure 9 compares the behavior of the quantity $L(\boldsymbol{e}, E)$ and of the estimate η_L versus the number of degrees of freedom, as the mesh is refined. The exact error quantity $L(\boldsymbol{e}, E)$ is actually unknown for the finite element solutions $(\boldsymbol{u}_h, p_h)$. Therefore, $L(\boldsymbol{e}, E)$ is approximated by the numerical quantity $L(\tilde{\boldsymbol{u}} - \boldsymbol{u}_h, \tilde{p} - p_h)$, where $(\tilde{\boldsymbol{u}}, \tilde{p})$ is the solution obtained on a finely refined mesh. This confirms that the estimate η_L is smaller by several orders of magnitude than the exact error quantity $L(\boldsymbol{e}, E)$. We can take advantage of the iterative adaptive procedure to extract a better estimate of the error. Let $\boldsymbol{u}_h^r$ defines a finite element solution after the r-th refinement level, $r = 0$ referring to the initial mesh. The error $L(\boldsymbol{e}, E)$ with respect to the solution $\boldsymbol{u}_h^r$ can then be approximated using the following quantity:

$$\tilde{\eta}_L = \left| L(\boldsymbol{u}_h^{r+1}, p_h^{r+1}) - L(\boldsymbol{u}_h^r, p_r^h) \right|. \tag{6.37}$$

The quantity $\tilde{\eta}_L$ is compared with $L(\boldsymbol{e}, E)$ in Figure 10.

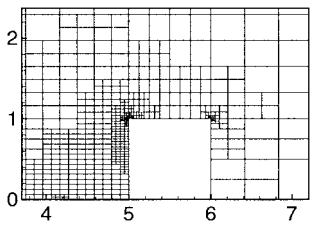

Figure 7. Adapted mesh with 881 elements.

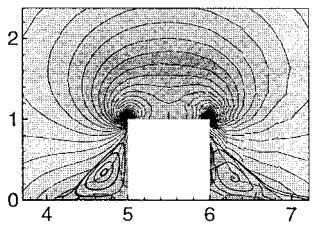

Figure 8. Vorticity contours and streamlines associated with the mesh of Figure 7.

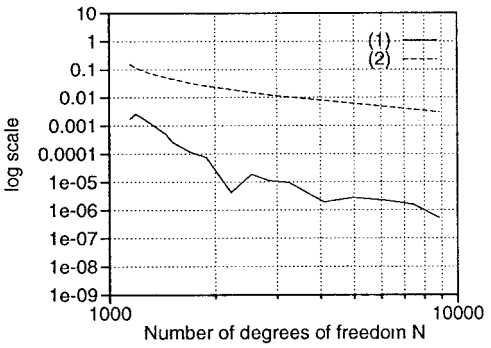

Figure 9. Comparison of $|L(\boldsymbol{e}, E)|$ (1) and η_L (2) versus the total number of degrees of freedom.

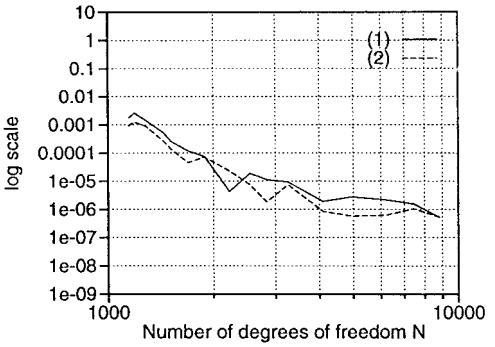

Figure 10. Comparison of $|L(e, E)|$ (1) and $\tilde{\eta}_L$ (2) versus the total number of degrees of freedom.

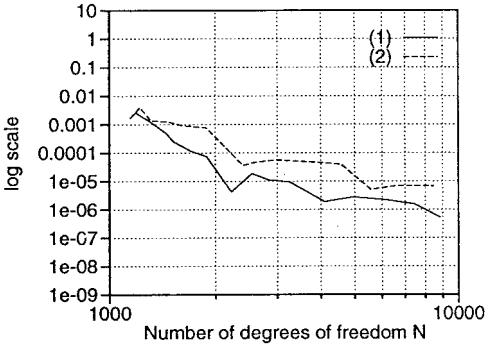

Figure 11. Evolution of the error $|L(e, E)|$ as the mesh is adapted using either the estimate η_L of $L(e, E)$ (1) or the estimate η_u of $(|e|_1^2 + \|E\|_0^2)^{1/2}$ (2).

Figure 11 shows the evolution of the error $L(e, E)$ with respect to the number of degrees of freedom when the mesh is refined using the two adaptative strategies. It confirms that the goal-oriented adaptive strategy accelerates the calculation of features of the solution to preset levels of accuracy as compared with traditional adaptive schemes based on global estimates.

7. SUMMARY AND CONCLUSIONS

We have presented an adaptive strategy to control computational processes with respect to linear functionals of the solution (u, p) of the Stokes and Oseen equations. The method involves the approximation of influence functions which are shown to be solutions of the dual problem and depends on obtaining reliable error estimators in the 'energy' norms for the Stokes and Oseen equations. We note in conclusion that the methodology can be extended by linearization to non-linear quantities of interest and to non-linear problems such as the steady state Navier–Stokes equations.

ACKNOWLEDGMENTS

The support of this work by the Office of Naval Research under contract N00014-95-1-0401 is gratefully acknowledged.

REFERENCES

1. I. Babuška, T. Strouboulis, C.S. Upadhyay and S.K. Gangaraj, '*A posteriori* estimation and adaptive control of the pollution error in the *h*-version of the finite element method', *Int. J. Numer. Methods Eng.*, **38**, 4207–4235 (1995).
2. R. Becker and R. Rannacher, 'Weighted *a posteriori* error control in FE method', in *ENUMATH-95*, Paris, September, 1995.
3. M. Paraschivoiu, J. Peraire and A.T. Patera, '*A posteriori* finite element bounds for linear-functional outputs of elliptic partial differential equations', *Comp. Methods Appl. Mech. Eng.*, **150**, 289–312 (1997).
4. J.T. Oden and S. Prudhomme, 'A technique for *a posteriori* error estimation of *h–p* approximations of the Stokes equations', in P. Ladevèze and J.T. Oden (eds), *Advances in Adaptive Computational Methods in Mechanics*, Elsevier, Amsterdam, 1998, pp. 43–63.
5. V. Girault and P.-A. Raviart, *Finite Element Methods for Navier–Stokes Equations*, Springer-Verlag, Berlin, 1986.
6. L. Demkowicz, J.T. Oden, W. Rachowicz and O. Hardy, 'Toward a universal *h–p* adaptive finite element strategy. Part 1. Constrained approximation and data structure', *Comp. Methods Appl. Mech. Eng.*, **77**, 113–180 (1989).
7. R.E. Bank, 'Hierarchical bases and the finite element method', *Acta Numerica*, **5**, 1–43 (1996).
8. J.T. Oden, 'Optimal *h–p* finite clement methods', *Comp. Methods Appl. Mech. Eng.*, **112**, 309–331 (1994).
9. B. Szabó and I. Babuška, *Finite Element Analysis*, John Wiley & Sons, New York, 1991.
10. M. Ainsworth and J.T. Oden, 'A unified approach to a posteriori error estimation using element residual methods', *Numer. Math.*, **65**, 23–50 (1993).
11. M. Ainsworth and J.T. Oden, '*A posteiori* error estimation in finite element analysis', *Comput. Methods Appl. Mech. Eng.*, **142**, 1–88 (1997).
12. P. Ladevèze and D. Leguillon, 'Error estimate procedure in the finite element method and applications', *SIAM J. Numer. Anal.*, **20**, 485–509 (1983).
13. M. Paraschivoiu and A.T. Patera, '*A posteriori* bounds for linear-functional outputs of Crouzeix–Raviart finite element discretizations of the incompressible Stokes problem', preprint.
14. J. Simo and F. Armero, 'Unconditional stability and long-term behavior of the transient algorithms for the incompressible Navier–Stokes and Euler equations', *Comp. Methods Appl. Mech. Eng.*, **111**, 111–154 (1994).
15. V.P. Fragos, S.P. Psychoudaki and N.A. Malamataris, 'Computer-aided analysis of flow past a surface-mounted obstacle', *Int. J. Numer. Methods Fluids*, **25**, 495–512 (1997).

